JOURNAL OF CATALYSIS 154, 230–244 (1995)

Formaldehyde Oxidation over Ag Catalysts

Ching-Feng Mao and M. Albert Vannice[1]

Department of Chemical Engineering, Pennsylvania State University, University Park, Pennsylvania 16802

Received October 11, 1994; revised March 8, 1995

H_2CO oxidation was studied over Ag powder, high surface area (HSA) α-alumina, and Ag dispersed on both (HSA) α-Al_2O_3 and SiO_2. Ag powder was active above 473 K with reaction orders of unity for O_2 and zero for H_2CO. All the supported Ag catalysts were active, even below 473 K, but significant deactivation occurred initially at the lower temperatures. Above 473 K the reaction orders for the supported Ag catalysts were near 0.3 for both O_2 and H_2CO. Turnover frequencies were determined for these Ag catalysts for the first time. Unlike silica, the (HSA) α-aluminas exhibited significant activity above 473 K. In addition to CO_2, CO was also a product above 493 K in the presence of alumina, probably due to the decomposition of formate species on the alumina surfaces. The IR spectra for H_2CO adsorption on alumina showed that formate groups dominated while significant amounts of dioxymethylene also existed at 303 K. At higher temperatures, dioxymethylene decomposed or oxidized to form formate groups. The spectra for H_2CO adsorption on a (HSA) α-alumina-supported Ag catalyst were similar to those for alumina, but a decrease in the formate species was observed after introducing oxygen at 493 K. Formate species were observed on the silica-supported Ag catalyst and were associated with H_2CO adsorption on oxygen-covered Ag; introduction of O_2 at 493 K after dosing with H_2CO resulted in the formation of gas-phase CO_2. A reaction model that assumes O_2 adsorption and formate decomposition to CO_2 to be the two slow steps provided excellent fits for the data for all catalysts.

INTRODUCTION

Formaldehyde is one of the major pollutants in the exhaust of methanol-fueled vehicles, and it can also be released from urea-formaldehyde resins which are used in a variety of consumer products. Since the carcinogenicity of formaldehyde was reported (1), concerns about its toxicity have increased and methods of formaldehyde detoxification have been examined. Catalytic combustion of formaldehyde is one of the methods that can effectively remove formaldehyde from the air. Several studies have reported on the oxidation of formaldehyde over supported metal catalysts or metal oxides (2–8); however, few kinetic data were obtained and limited information about surface species under reaction conditions is available. Therefore, the aim of this study was to examine the kinetic behavior of H_2CO oxidation over supported metal catalysts and to investigate the adsorbed H_2CO species. High surface area (HSA) α-alumina-supported Ag catalysts were chosen because they have been shown to be very active for acetaldehyde oxidation and have been well characterized (9); consequently, they are promising candidates for efficient formaldehyde oxidation.

At room temperature gaseous formaldehyde easily polymerizes to paraformaldehyde, which can revert to gaseous formaldehyde to an appreciable extent when the temperature rises above certain levels. Therefore heating paraformaldehyde provides a convenient source of pure gaseous formaldehyde; however, methods other than this have been used in past studies of H_2CO oxidation over supported metals. For example, McCabe and Mitchell employed a prereactor to produce formaldehyde by the partial oxidation of methanol to simulate vehicle exhaust in which methanol and CO were also present (2). Imamura *et al.* investigated formaldehyde oxidation over CeO_2-supported precious metals using aqueous formaldehyde containing methanol as a stabilizer in the feed (3, 4). Reactors other than steady-state, packed-bed reactors have also been used, such as a batch reactor containing solid paraformaldehyde (5) or a semibatch reactor with oxygen flowing through an aqueous solution of formaldehyde (6). The only studies for H_2CO oxidation with pure gaseous formaldehyde were performed with a Pt wire (7) and nickel oxide (8). In view of the previous studies, in which no kinetic data were obtained over supported metal catalysts using a differential reactor with only H_2CO and O_2 as reactants, an investigation of the kinetic behavior of H_2CO oxidation under reaction conditions involving only formaldehyde and O_2 clearly was warranted.

These experiments were carried out by warming paraformaldehyde in a temperature bath under flowing helium to generate a steady-state partial pressure of gas-phase formaldehyde. Reaction kinetics were examined between 373 and 523 K over Ag powder, (HSA) α-alumina or silica-supported Ag catalysts, and the pure supports using a differential reactor. These Ag catalysts were character-

[1] To whom correspondence should be addressed.

0021-9517/95 $12.00

ized by oxygen chemisorption and hydrogen titration in a high-vacuum adsorption system. In addition, diffuse reflectance FTIR (DRIFTS) was employed to study the evolution of adsorbed species during formaldehyde adsorption and oxidation.

EXPERIMENTAL

Catalyst Preparation

All the supported Ag catalysts, except for the 1.5% Ag/SiO_2 sample, were prepared by an incipient wetness method using $AgNO_3$ (Aldrich Co., 99.9999%) dissolved in doubly distilled, deionized water followed by drying at 383 K in an oven and storage in a desiccator. The support materials used were two high surface area (HSA) aluminas—α-Al_2O_3(U) (Alcoa, 78 $m^2\ g^{-1}$) and α-Al_2O_3(G) (Alcoa, 104 $m^2\ g^{-1}$)—which were prepared from unground and ground diaspore, respectively (10), and SiO_2 (Davison, grade 57, 220 $m^2\ g^{-1}$, 60–80 mesh). In order to achieve high Ag dispersions, the 1.5% Ag/SiO_2 sample was prepared by an ion-exchange method with this SiO_2 (<100 mesh) (11). All supports were heated at 823 K for 2 h in air (Linde, dry grade) at 500 cm^3 (STP) min^{-1} prior to impregnation or ion-exchange with Ag. The Ag loadings were determined by plasma emission spectroscopy at the Mineral Constitution Laboratory of Pennsylvania State University, except for the 16.65% Ag/SiO_2 catalyst, which was analyzed at the Dow Chemical Company. Ag powder (Johnson Matthey, Puratronic, 99.9995%) was used for studies over unsupported Ag.

Catalyst Characterization

The number of surface Ag atoms was measured by both oxygen chemisorption and hydrogen titration at 443 K in a stainless steel adsorption system with an ultimate vacuum of 10^{-8} Torr, which has been described previously (12). The pretreatment consisted of calcination in 10% O_2/90% He (40 cm^3 (STP) min^{-1}) at 773 K for 2 h followed by reduction in H_2 (20 cm^3 (STP) min^{-1}) at 673 K for 2.5 h and was carried out *in situ* prior to chemisorption measurements. H_2 (MG Ind. 99.999%) and He (MG Ind., 99.999%) were flowed through molecular sieve traps and Oxytraps (Alltech) while O_2 (MG Ind., 99.999%) was passed through a molecular sieve trap.

Catalytic Measurements

Kinetic studies were conducted in the vapor phase at atmospheric pressure in a Pyrex reactor which was placed inside a heating mantle equipped with a temperature controller. *In situ* pretreatments identical to those employed in the chemisorption measurement were carried out before the introduction of reactants. A continuous flow of gaseous formaldehyde was established by passing a carrier gas through a glass flask containing paraformaldehyde (Aldrich, 95%) which was situated in a temperature bath (Fisher Scientific, Model 90) held at temperatures from 338 to 353 K, while all the tubing after this formaldehyde generator and the GC sampling valve were heated to 390 K to prevent recondensation of formaldehyde. The flow rate of formaldehyde was calibrated by passing the formaldehyde-containing gas into doubly distilled, deionized water and analyzing the resulting solution by the sulfite method (13), and the partial pressure of formaldehyde determined from these measurements was then controlled by heating paraformaldehyde at different temperatures while the flow rates of O_2 and He were regulated by mass flow controllers (Tylan, FC-260). Typically a total feed flow rate of 10 cm^3 (STP) min^{-1} containing 1.2% formaldehyde and 14.8% O_2 (balance He) was passed through the reactor containing either 50 mg of supported Ag catalyst or 1 g of Ag powder, corresponding to a space velocity of either 7000 or 1000 h^{-1}. The reaction to form CO_2 or CO was studied from 373 to 513 K, and the data were acquired in an ascending temperature sequence followed by a descending temperature sequence to detect any deactivation. Partial pressure dependencies on formaldehyde were typically determined at an O_2 composition of 14.8%, while those on O_2 were determined at a formaldehyde composition of 1.2%. An ascending partial pressure of O_2 or formaldehyde followed by descending partial pressure was also employed to detect deactivation over these supported Ag catalysts and aluminas. The activity was measured after a period of 20 min on stream following each change in temperature or flow composition. Product analysis was conducted with a gas chromatograph (Hewlett Packard, 5730A) equipped with a Carboxen^{1000} column (Supelco). The maximum conversions were around 20%, while most conversions were kept below 10% so that a differential reactor could be assumed. On the alumina-supported Ag catalysts, a satisfactory carbon balance could not be obtained due to the adsorption or polymerization of formaldehyde on the alumina surface.

DRIFTS Study

The infrared studies were conducted using a N_2-purged FTIR spectrometer (Mattson Instr., RS-10000) equipped with a DRIFTS cell (Harrick Scientific, HVC-DR2) in conjunction with a praying mantis mirror assembly (Harrick Scientific, DRA-2C0). Modifications were made to facilitate height adjustment outside the sample chamber and to allow the temperature within the catalyst bed to be measured. Some of these have been described earlier (14); however, a different apparatus for height adjustment was used here. It consisted of a lever attached through a transparent acrylic sample chamber cover to move the height adjuster of the DRIFTS cell. Catalysts were ground

(<325 mesh) and loaded into the cell, and the same *in situ* pretreatment was employed before the introduction of reactants, except that the calcination temperature was 673 K. The formaldehyde partial pressure was generated as before; however, formaldehyde was now manually introduced by pulses from a six-port switching valve instead of by a steady flow to prevent excessive formaldehyde condensation on the DRIFTS cell wall. Pulses of formaldehyde (ca. 0.43 μmol H_2CO per pulse) were introduced to the cell with flowing He (10 cm^3 (STP) min^{-1}) or a mixture of 15% O_2/85% He (10 cm^3 (STP) min^{-1}) at 303, 393, and 493 K. Interferograms were obtained by averaging 100 scans at a resolution of 4 cm^{-1} after the introduction of each pulse of formaldehyde.

RESULTS

O_2 Chemisorption and H_2 Titration

Table 1 lists O_2 chemisorption and H_2 titration uptakes at 443 K along with Ag dispersions, as defined by H_2 titration, i.e., dispersion = $Ag_{surf}/Ag_{total} = H_{2\,titr}/Ag_{total}$ or $O_{ad}/Ag_{surf} = 1$. As expected, Ag powder had much lower gas uptakes and thus a much larger particle size than the supported Ag catalysts. The dispersions of the (HSA) α-alumina-supported samples were higher than those of the silica-supported samples. The H_{titr}/O_{ad} titration ratios for Ag powder and the (HSA) α-alumina-supported samples were close to two, as expected (12), but a larger deviation existed with the silica-supported samples.

Kinetic Study

The activities of the Ag catalysts and the (HSA) α-alumina for H_2CO oxidation to CO_2 at P_{O_2} = 112 Torr and P_{H_2CO} = 9 Torr (1 Torr = 133.3 kPa) are shown by the Arrhenius plots in Fig. 1. Activity over the Ag powder was not observed below 470 K but could be measured

TABLE 1

Oxygen Adsorption and Hydrogen Titration on Silver Catalysts at 443 K

Catalyst	Gas uptake (μmol/g cat) O_2	Gas uptake (μmol/g cat) H_2 titr.	Initial dispersion[a] (Ag_{surf}/Ag_{total})	d[b] (nm)
Ag powder	0.65	1.21	0.00013	10,000
0.83% Ag/α-Al_2O_3(U)	16.5	33.0	0.43	3.1
0.71% Ag/α-Al_2O_3(G)	18.4	34.7	0.53	2.5
1.5% Ag/SiO_2	13.8	34.8	0.25	5.4
16.65% Ag/SiO_2	72.8	126.2	0.082	16.4

[a] Based on H_{2titr}/Ag_{total} = dispersion, i.e., Ag–O + $H_2 \rightarrow$ Ag + $H_2O_{(ad)}$ (Ref. 12).

[b] Calculated from d (nm) = 1.34/dispersion.

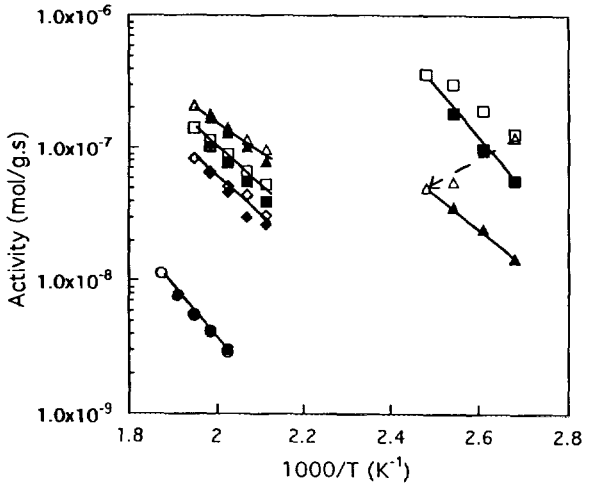

FIG. 1. Arrhenius plots of formaldehyde oxidation to CO_2 over Ag catalysts and aluminas at P_{O_2} = 112 Torr and P_{H_2CO} = 9 Torr; Ag powder (○, ●), 0.83% Ag/α-Al_2O_3(U) (□, ■), 1.5% Ag/SiO_2 (△, ▲), and α-Al_2O_3(U) (◇, ◆). Open symbols represent an ascending temperature sequence and solid symbols represent a descending temperature sequence. Dashed line represents initial deactivation of 1.5% Ag/SiO_2.

above 473 K, and it exhibited a reversible temperature dependency without deactivation, as shown by the Arrhenius plot. The supported Ag samples also showed little deactivation above 473 K, but had noticeably higher activity below 473 K when freshly reduced catalysts were initially tested. For the supported Ag catalysts below 473 K, rapid deactivation occurred, as shown by the Arrhenius plots in Fig. 1, and the activity of the silica-supported Ag sample decreased to such a low level that CO_2 was almost not measurable after the descending temperature sequence. The extent of deactivation during the rate measurements could be estimated by the percent of activity decrease in the Arrhenius plots at 373 K, and this gave activity losses in this low temperature region of 56% for 0.83% Ag/α-Al_2O_3(U), 62% for 0.71% Ag/α-Al_2O_3(G), and 88% for 1.5% Ag/SiO_2, thus showing that the deactivation on the silica-supported sample was more pronounced than that on the (HSA) α-alumina-supported samples. A calcination treatment at 773 K in a mixture of 10% O_2 and He followed by reduction in H_2 at 673 K did not recover the activity below 473 K, so activity measurements were then conducted above 473 K. Deactivation also occurred above this temperature, but was milder compared to that below 473 K, as revealed by the extent of deactivation estimated by the percent of activity decrease at 473 K during the rate measurements, which was 27% for 0.83% Ag/α-Al_2O_3(U), 37% for 0.71% Ag/α-Al_2O_3(G), and 18% for 1.5% Ag/SiO_2. In contrast to the deactivation below 473 K, the silica-supported sample now had the lowest deactivation among the three supported Ag catalysts. The pure (HSA) α-Al_2O_3 samples were also active above 473 K, with activities lower than but on the same order

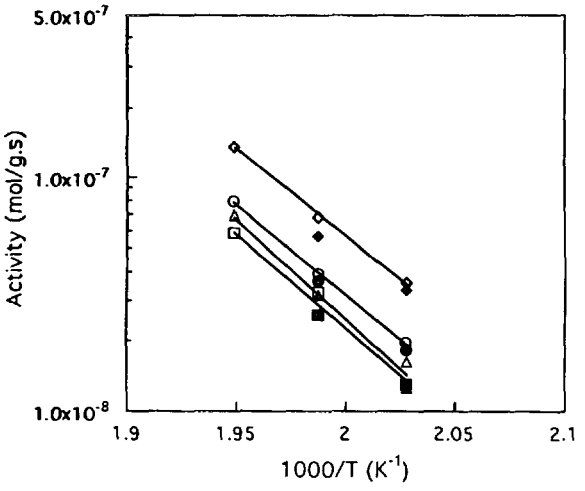

FIG. 2. Arrhenius plots of formaldehyde oxidation to CO over Ag catalysts and aluminas at P_{O_2} = 112 Torr and P_{H_2CO} = 9 Torr: 0.83% Ag/α-Al_2O_3(U) (○, ●), 0.71% Ag/α-Al_2O_3(G) (□, ■), α-Al_2O_3(U) (△, ▲), and α-Al_2O_3(G) (◇, ◆). Open symbols represent an ascending temperature sequence and solid symbols represent a descending temperature sequence.

of magnitude as those of the corresponding supported Ag samples; thus the overall activity of the (HSA) α-alumina-supported Ag samples includes the reaction on the alumina surface. Deactivation was likewise observed over these (HSA) α-aluminas, where the extent of deactivation was 14% for α-Al_2O_3(U) and 69% for α-Al_2O_3(G). No measurable activity was detected with pure silica, so the activity of the silica-supported sample on Ag surfaces can be attributed to H_2CO oxidation only.

CO was also produced during H_2CO oxidation above 493 K over the (HSA) α-alumina-supported Ag catalysts and the (HSA) α-aluminas, and the Arrhenius plots for the production of CO at P_{O_2} = 112 Torr and P_{H_2CO} = 9 Torr are shown in Fig. 2. In contrast, CO was not observed over either Ag powder or the Ag/SiO_2 sample. The deactivation for CO formation was slight compared to that for CO_2. Since the activity for CO formation on the aluminas was always higher than that on the (HSA) α-alumina-supported Ag catalysts, and since Ag powder did not produce CO, it is assumed that CO was primarily produced on the alumina surfaces of the (HSA) α-alumina-supported Ag catalysts, with the resulting CO possibly being further oxidized on the Ag surface, as Ag is known to be active for CO oxidation (15, 16).

As indicated in Fig. 1, the catalytic behavior in the temperature region below 473 K was different than that above 473 K, thus kinetic results are given separately for each region in Tables 2 and 3. In both tables, initial activities represent values in the ascending temperature sequence, but the apparent activation energies (E_a) in Table 2 are derived only from the slope of the descending temperature sequence, to minimize any effect of deactivation, whereas average values of E_a are given in Table 3. Turnover frequencies (TOF) are based on the initial dispersions given in Table 1. For formaldehyde oxidation below 473 K, the 0.71% Ag/α-Al_2O_3(G) had a somewhat

TABLE 2

Formaldehyde Oxidation Kinetics at Temperatures below 443 K

Catalyst	Initial activity at 373 K[a]		E_a (kJ/mol)[b]
	r (mol/g·s × 10^7)	TOF (s^{-1} × 10^3)	
0.83% Ag/α-Al_2O_3(U)	1.3	3.9	78
0.71% Ag/α-Al_2O_3(G)	0.81	2.3	74
1.5% Ag/SiO_2	1.2	3.5	50

Note. Reaction Conditions: P_{O_2} = 112 Torr and P_{H_2CO} = 9 Torr.
[a] Only CO_2 formed.
[b] Obtained from descending temperature sequence.

TABLE 3

Formaldehyde Oxidation Kinetics at Temperatures above 443 K

Catalyst	S^a (%)	Activity at 493 K[b]		E_a (kJ/mol)		Reaction order[b]	
		r (mol/g·s × 10^7)	TOF (s^{-1} × 10^3)	CO_2	CO	O_2	H_2CO
Ag powder	100	0.030	2.5	71	—	0.95	0
0.83% Ag/α-Al_2O_3(U)[c]	82	0.88	1.1[d]	57	148	0.27	0.22
0.71% Ag/α-Al_2O_3(G)[c]	92	1.53	3.2[d]	51	160	0.25	0.34
1.5% Ag/SiO_2[c]	100	1.39	4.0	44	—	0.32	0.32
α-Al_2O_3(U)	76	0.52	—	55	165	0.10	0.36
α-Al_2O_3(G)	46	0.41	—	62	145	0.11	0.61

[a] Selectivity at 493 K, defined as mol CO_2/(mol CO_2 + mol CO).
[b] For CO_2 formation.
[c] Samples after deactivation below 473 K were used.
[d] After correction for the contribution from aluminas.

lower TOF than the other two Ag catalysts, but the activation energies of the two (HSA) α-alumina-supported samples were nearly identical and were larger than that for the Ag/SiO_2 catalyst, as shown in Table 2. In Table 3, the TOFs for CO_2 formation above 473 K on the Ag/(HSA) α-Al_2O_3 catalysts were corrected for the contribution from the support. The Ag/SiO_2 catalyst was the most active and still had the lowest E_a, while the TOFs of the (HSA) α-alumina-supported Ag samples were more similar to that for Ag powder. Since CO was also generated in this temperature region, selectivity to CO_2 is defined as mole CO_2/(mole CO_2 + mole CO) × 100. The selectivity of supported Ag catalysts was always higher than that of the supports alone. The activation energy for CO formation (145–165 kJ mol^{-1}) was about two times higher than that for CO_2; consequently, at higher temperatures the selectivity significantly decreased.

The partial pressure dependencies on O_2 and H_2CO for formaldehyde oxidation to CO_2 above 473 K were studied at 493 K after the rates vs temperature curves were obtained, as shown in Figs. 3 and 4, and the results from a power rate law fit are listed in Table 3; however, the dependencies below 473 K were not investigated due to significant deactivation. For Ag powder the reaction order of O_2 was near unity and that of H_2CO was zero, while for the supported Ag catalysts the reaction orders with respect to both O_2 and H_2CO were usually around 0.3, regardless of the support. For the (HSA) α-aluminas the reaction order of O_2 was close to 0.10, which was lower than that of the Ag catalysts, while the reaction order of H_2CO was higher compared to that of the Ag catalysts. A correction of the activity in the partial pressure dependency studies for the contribution from the support for the Ag/α-Al_2O_3 samples was attempted, but it was not successful because of the presence of deactivation.

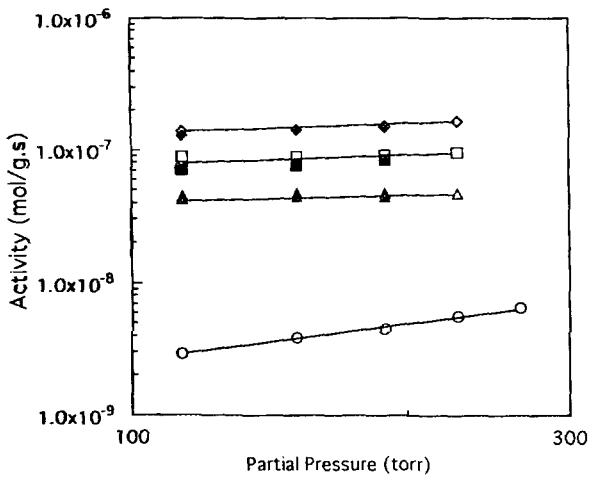

FIG. 3. Dependence of formaldehyde oxidation on O_2 pressure over Ag catalysts and aluminas at 493 K: Ag powder (○), 0.83% Ag/α-Al_2O_3(U) (□, ■), α-Al_2O_3(U) (△, ▲), and 1.5% Ag/SiO_2 (◇, ◆). Open symbols represent an ascending pressure sequence and solid symbols represent a descending pressure sequence.

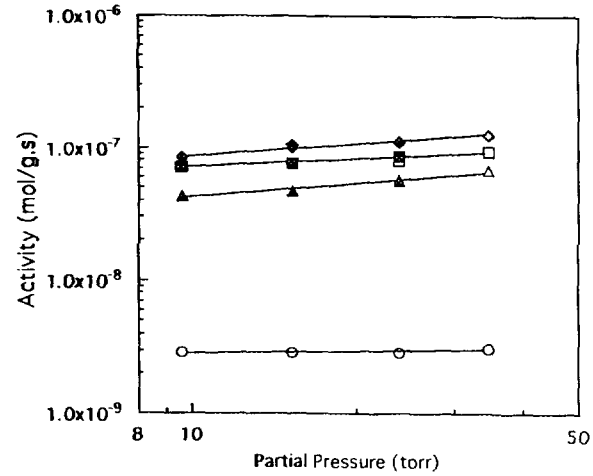

FIG. 4. Dependence of formaldehyde oxidation on H_2CO pressure over Ag catalysts and aluminas at 493 K: Ag powder (○), 0.83% Ag/α-Al_2O_3(U) (□, ■), α-Al_2O_3(U) (△, ▲), and 1.5% Ag/SiO_2 (◇, ◆). Open symbols represent an ascending pressure sequence and solid symbols represent a descending pressure sequence.

Infrared Study

The IR spectra of silica after exposure to H_2CO, referenced to a clean pretreated surface, showed no bands developing even at 303 K, thus indicating that little or no H_2CO adsorbs onto silica surfaces above 303 K. This result differs from that reported for H_2CO adsorption on an Aerosil silica in a static system in which polyoxymethylene (POM) species were observed at room temperature (the pressure of H_2CO was not specified in this paper) (17); however, this difference is probably due to the very low concentration of H_2CO in each pulse, which cannot generate high enough concentrations on the surface to allow condensation of H_2CO to POM, plus the fact that H_2CO was introduced at 170 K in the study by Busca *et al.* Nevertheless, the fact that no dioxymethylene or formate species have been reported in the literature after H_2CO adsorption on silica suggests that the interaction between silica and H_2CO is weak. Because there are no IR features attributable to H_2CO adsorbed on silica, any spectra obtained with the silica-supported Ag catalyst can be directly related to adsorbed species on Ag; however, no bands were observed with a freshly reduced 1.5% Ag/SiO_2 sample after introducing H_2CO in either the presence or the absence of O_2. This may have been due to the low Ag loading in this sample. The 1.5% Ag/SiO_2 sample used in the kinetic study was taken from the reactor, loaded into the DRIFTS cell, and purged with He at 493 K, which caused little significant change in the spectrum. Four pulses of H_2CO in He were then intro-

duced at 493 K and again no significant bands developed, a result similar to that observed with the freshly reduced sample. Oxygen was introduced after this dosing of H_2CO, and the band strength at 1710 cm^{-1} decreased while gas-phase CO_2 (identified by the two bands near 2340 and 2360 cm^{-1}) was initially produced then disappeared, as shown in Figs. 5b–5e. The band at 1710 cm^{-1} is assigned to a weakly adsorbed H_2CO species because of the similarity to a band at 1735 cm^{-1} for gas-phase H_2CO (18); this species is probably associated with the Ag surface because the C=O stretching band at 1710 cm^{-1} is the same as that reported for H_2CO on Ag(110) (19). A study of H_2CO adsorption on oxygen-covered low-surface-area Ag powder was also conducted, but no bands associated with adsorbed species could be detected (20).

Formaldehyde adsorption on a catalyst with higher silver loading, 16.65% Ag/SiO_2, was then studied in an effort to enhance detection of the adsorbed species on the Ag surface. After pretreatment, a flow of 15% O_2 in He was introduced at 443 K to generate an oxygen-covered Ag surface. Formaldehyde was then dosed at 303 K in He and a weak band at 1610 cm^{-1} developed, as shown in Fig. 6a. Further dosing of H_2CO at 393 K did not change this band, but when the temperature was raised to 493 K, the band shifted to 1595 cm^{-1} and two broad bands formed around 1380 and 990 cm^{-1} (Fig. 6b). Further dosing of H_2CO at 493 K had no effect on these bands, but after exposure to oxygen at 493 K, the band at 1595 cm^{-1} shifted to 1585 cm^{-1} and broadened, and CO_2 formation was now observed, as shown in Fig. 6c. The structures of possible adsorbed species are shown in Fig. 7. The weak band at 1610 cm^{-1} is attributed to the asymmetric COO stretching mode of formate species on Ag surfaces (Fig. 7b), based on the studies of formic acid adsorption on Ag(110) and supported Ag catalysts (21, 22). The absence of a band for a CH stretching mode around 2900 cm^{-1} may be due to a smaller extinction coefficient and the low concentration of these formate species. For those bands present at 493 K, the bands at 1595 and 1380 cm^{-1} can be attributed to the asymmetric and symmetric COO stretching vibrations, respectively, of formate groups (19, 21, 22), though they have also been assigned to features of bicarbonate groups (4). The band at 1595 cm^{-1} was accompanied by some surrounding perturbation, which is attributed to gas-phase water as a product of formaldehyde oxidation at 493 K. Bands around 990 cm^{-1} have not yet been assigned in the literature to any particular mode of formate groups on Ag; however, the monodentate acetate group in $[Pd(ac)_2(PPh_3)]_2$ has three COO deformation bands between 720–920 cm^{-1} in addition to two bands at 1629 and 1314 cm^{-1}. These former bands are reduced in number in bidentate complexes (23). Consequently, the bands between 900–1000 cm^{-1} are tentatively assigned to formate species, including a possible monodentate structure, as shown in Fig. 7c. Bands between 700–800 cm^{-1} have also been associated with adsorbed H_2O (21). Table 4 lists the assignments of the IR bands associated with H_2CO adsorption on silica-supported Ag.

The spectra for H_2CO adsorption on α-alumina were much more complicated and presented numerous strong adsorption bands. Both a fresh α-Al_2O_3(U) sample and a sample that had been used in the kinetic runs were

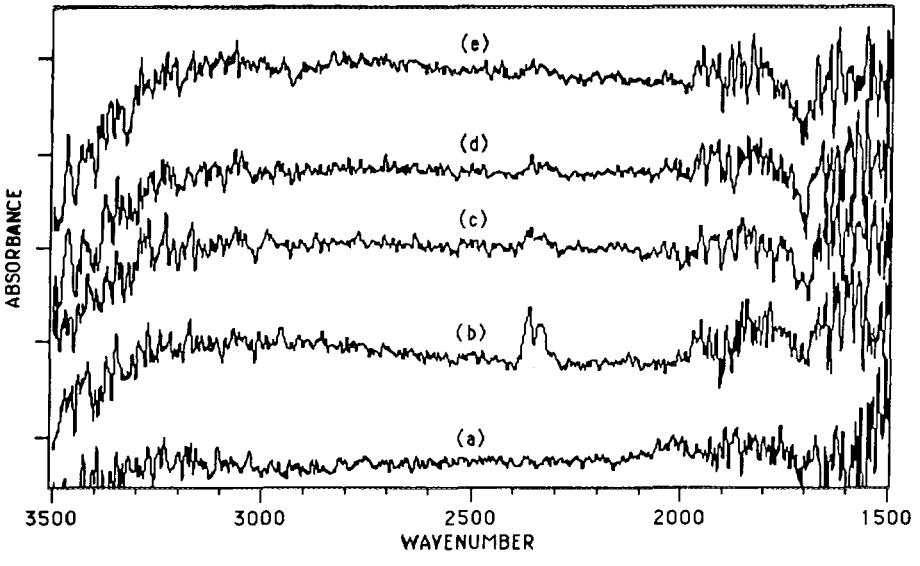

FIG. 5. DRIFT spectra of 1.5% Ag/SiO_2 (sample after kinetic study) after exposure to 4 pulses of formaldehyde: (a) 40 min after raising temperature to 493 K in He; (b) 2 min after exposure to O_2 at 493 K; (c) after 10 min, same conditions as b; (d) after 20 min, same conditions as b; and (e) after 30 min, same conditions as b. The reference spectrum for (a) is that of the initial sample at 493 K, and the reference spectrum for (b)–(e) is that after the last dose of H_2CO at 493 K. Scale: 1 division = 0.005 absorbance unit.

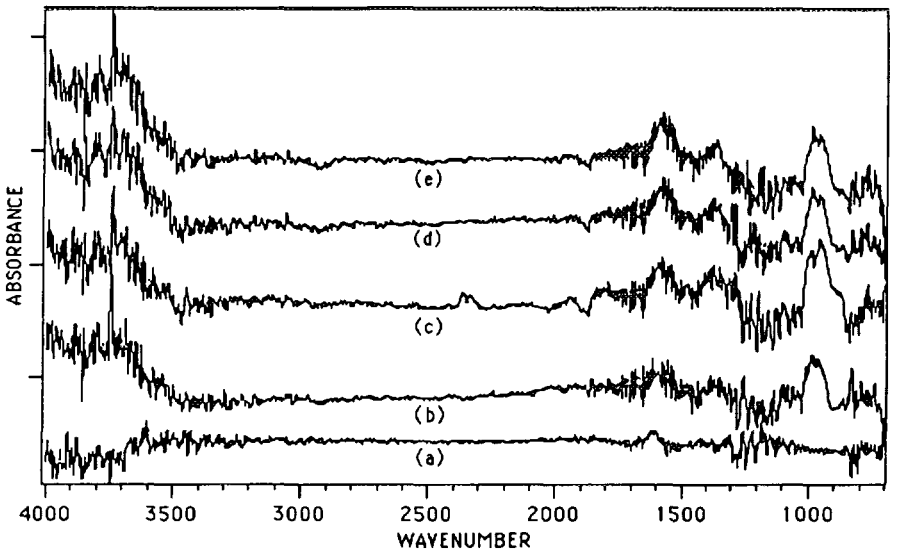

FIG. 6. DRIFT spectra of 16.65% Ag/SiO_2: (a) after exposure to four pulses of H_2CO in He at 303 K; (b) in He at 493 K after last dose of H_2CO at 393 K; (c) 2 min after exposure to O_2 at 493 K; (d) after 10 min at 493 K; and (e) after 30 min at 493 K. The reference spectrum is that of the sample prior to dosing H_2CO. Scale: 1 division = 0.02 absorbance unit. Gas-phase H_2O contributions have been subtracted.

investigated in the infrared studies, and the results are shown in Figs. 8–11. Figure 8 shows spectra for H_2CO adsorption on the fresh α-Al_2O_3(U) sample after the standard pretreatment under a mixture of 15% O_2 in He at 303 K. A loss in the OH stretching mode at 3730 cm^{-1} and the growth of bands around 2500–3000, 1620, 1595, 1300–1500, and 950–1150 cm^{-1} were observed. The doublet at 1620 and 1595 cm^{-1} was the strongest band. In order to interpret the spectra, these bands are roughly divided into two groups according to their different behaviors after dosing H_2CO at higher temperatures, as shown in Figs. 8 and 9. Group A includes the doublet at 1620 and 1595 cm^{-1}, as well as the band at 1390 cm^{-1}, while

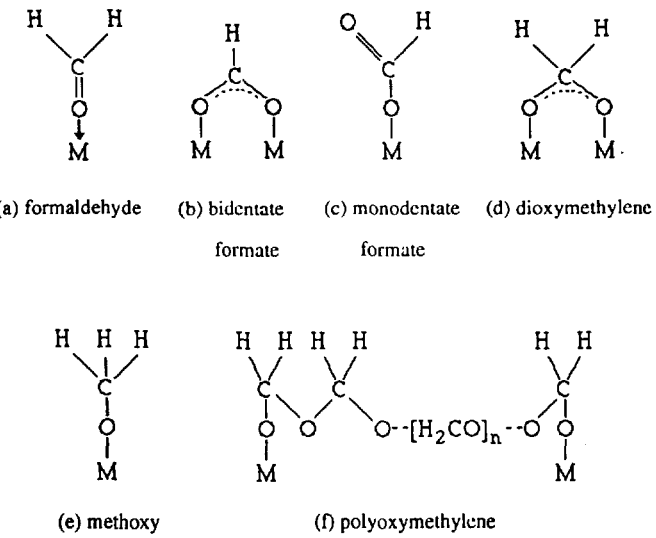

FIG. 7. Possible surface species formed from the adsorption of H_2CO onto Ag and Al_2O_3.

TABLE 4

Wavenumbers (cm^{-1}) of Species Associated with H_2CO Adsorption on Ag and α-Al_2O_3 and Their Assignments

Observed wavenumber (cm^{-1})	Assignment	Reference
	Ag/SiO_2	
	Formate (possibly monodentate) on Ag:	
990	COO deformation	(23, this study)
	Formate on Ag:	
1590–1610	COO asym. stretching	(21, 22)
1380	COO sym. stretching	(19, 21, 22)
	Formaldehyde on Ag:	
1710	C=O stretching	(18, 19)
	α-Al_2O_3	
	Formate:	
2900	CH stretching	(17, 25)
1595, 1620	COO asym. stretching	(17, 24, 25)
ca. 1400	CH bending	(17, 24, 25)
1370, 1410	COO sym. stretching.	(17, 24, 25)
2920–2955, 2850, 2745, 1460, 1435, 1300, 1135	Dioxymethylene	(17, 26)
2920, 2850, 1000	Methoxy	(17, 24)
1200, 1135	Polyoxymethylene (POM)	(17, 30–32)
1660	Water (adsorbed)	(33, 34)

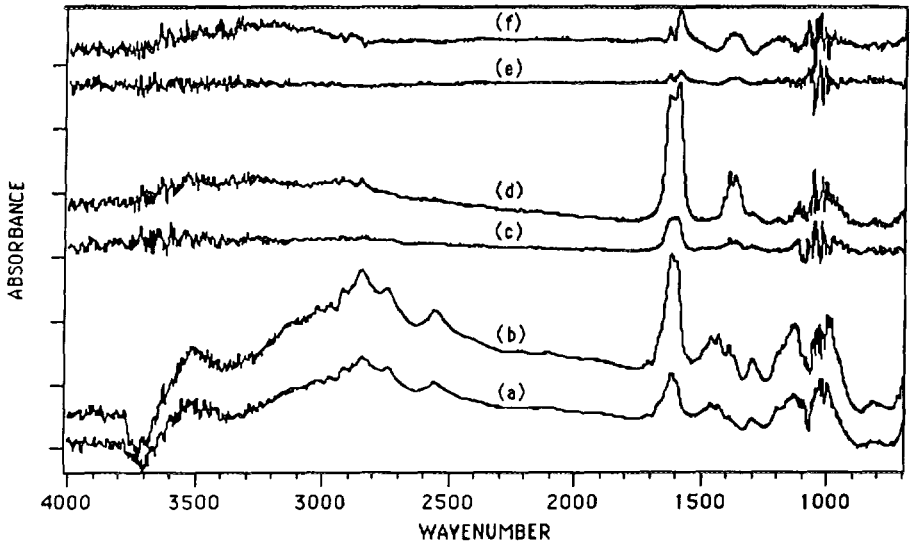

FIG. 8. DRIFT spectra of α-Al_2O_3(U) at 303 and 393 K after exposure to pulses of formaldehyde in 15% O_2 (balance He): (a) first H_2CO at 303 K; (b) fourth H_2CO at 303 K; (c) first H_2CO at 393 K; (d) fourth H_2CO at 393 K; (e) 10 min after fourth dose of H_2CO at 393 K; and (f) after 40 min at 393 K. The reference spectrum for (a) and (b) is that of the sample before dosing H_2CO at 303 K, for (c) and (d) it is the spectrum at 393 K following (b), and the reference spectrum for (e) and (f) is that of the sample after the last dose of H_2CO at 393 K. Scale: 1 division = 0.02 absorbance unit.

the remaining bands at 2920, 2850, 2745, 2560, 1460, 1435, 1300, 1135, and 1000 cm^{-1} constitute Group B. When H_2CO was dosed at 393 K, the bands in Group A steadily increased and two additional bands developed at 1410 and 1370 cm^{-1}, which are included in group A, while all the bands in Group B stopped growing except for those at 2850 and 1300 cm^{-1}, which appear as very weak bands in Fig. 8. Consequently, the bands in Group A are associated with the dominant organic species at 393 K. The evolution of peak intensities after the last dose of H_2CO at 393 K revealed that the bands in Group A were further enhanced, and a loss in band intensity at 2920, 2850, 1460, and 1300 cm^{-1} was observed for Group B. Figure 9 shows spectra during the dosing of H_2CO at 493 K, and again a

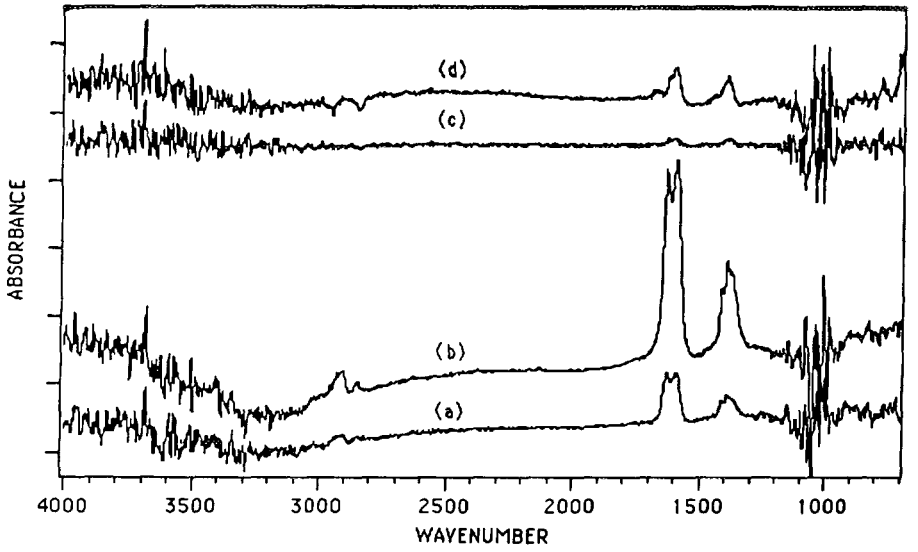

FIG. 9. DRIFT spectra of α-Al_2O_3(U) at 493 K after exposure to pulses of formaldehyde in 15% O_2 (balance He): (a) first H_2CO; (b) fourth H_2CO; (c) 20 min after last dose of H_2CO; and (d) after 60 min. The reference spectrum for (a) and (b) is that of the sample before dosing H_2CO, and the reference spectrum for (c) and (d) is that of the sample after the last dose of H_2CO. Scale: 1 division = 0.01 absorbance unit.

steady growth of Group A was the predominant feature while a band at 2900 cm^{-1} along with a weak, Group B band at 2850 cm^{-1} was also present. The evolution of peaks after the last dose of H_2CO at 493 K was similar to that at 393 K except that a loss of intensity at 2920 cm^{-1} was replaced by a loss at 2955 cm^{-1}.

The bands associated with Group A can be identified as features of a bidentate formate species with the peaks at 1620 and 1595 cm^{-1} assigned to the asymmetric COO stretching mode on two different sites and the bands at 1410 and 1370 cm^{-1} assigned to the symmetric COO stretching mode on these two sites, while the band at 2900 cm^{-1} can be assigned to the CH stretching mode (17, 24, 25); evidently, formate species are the dominant adsorbed species above 393 K. In contrast, interpretation of Group B is more difficult because it may be composed of several species. For the spectra at 303 K, all the bands in Group B, except those at 2560 and 1000 cm^{-1}, can be assigned to dioxymethylene species (17, 26) which, like the formate species, are also present in large amounts. The band at 1000 cm^{-1} is possibly due to methoxy groups whose CH_3 vibrations overlap those of the dioxymethylene species (17, 24). In contrast, the band at 2560 cm^{-1} can be assigned to redshifted OH stretching vibrations caused by H-bonding interactions (27–29). In addition, the existence of POM at 303 K cannot be ruled out since its characteristic bands at 1230 and 110 cm^{-1} are similar to the broad band at 1135 cm^{-1} with a shoulder around 1200 cm^{-1} (17, 30–32). The bands in Group B did not intensify at higher temperatures except for the weak bands at 2850 and 1300 cm^{-1}. The latter appeared as a shoulder at 393 K and corresponds to dioxymethylene species, while the former can be assigned to either dioxymethylene or methoxy species. Table 4 lists the assignments of the bands observed after H_2O adsorption on the α-Al_2O_3 surface. An experiment with fresh α-Al_2O_3(U) was also conducted with H_2CO pulses in pure He, instead of 15% O_2, and the results were similar to those obtained with an oxygen-containing flow (20).

The spectra for adsorbed species on the α-Al_2O_3(U) sample after completion of the kinetic studies were very different from those for H_2CO adsorbed on a fresh sample. Since the surface of the used sample was saturated with adsorbed species formed under reaction conditions, a harsh pretreatment was avoided in order to preserve these species; therefore, the sample was pretreated in flowing He at 493 K and the evolution of surface species with time was monitored. This is represented by the spectra in Fig. 10, which show incremental changes during successive time periods. During the first 1.5-h period, a broad band at 1030 cm^{-1} along with weaker bands at 1620, 1595, and 1415 cm^{-1} continued to grow while a decrease in band intensity at 2850 and 2730 cm^{-1} was observed; however, during the next 30 min, no further development occurred. Loss of band intensity at 1660 cm^{-1} may have occurred at the beginning but it overlapped the bands at 1620 and 1595 cm^{-1}. Dosing H_2CO at 493 K after this heating step enhanced the bands previously assigned to dioxymethylene, except in the 1000–1200 cm^{-1} region, and caused the growth of a broad band at 1660 cm^{-1}, as shown in Fig. 11a. The evolution of bands after the last dose of H_2CO was a reversal of that obtained during H_2CO dosing, and growth of bands associated with formate species can be recognized without ambiguity, as shown in Fig. 11. In

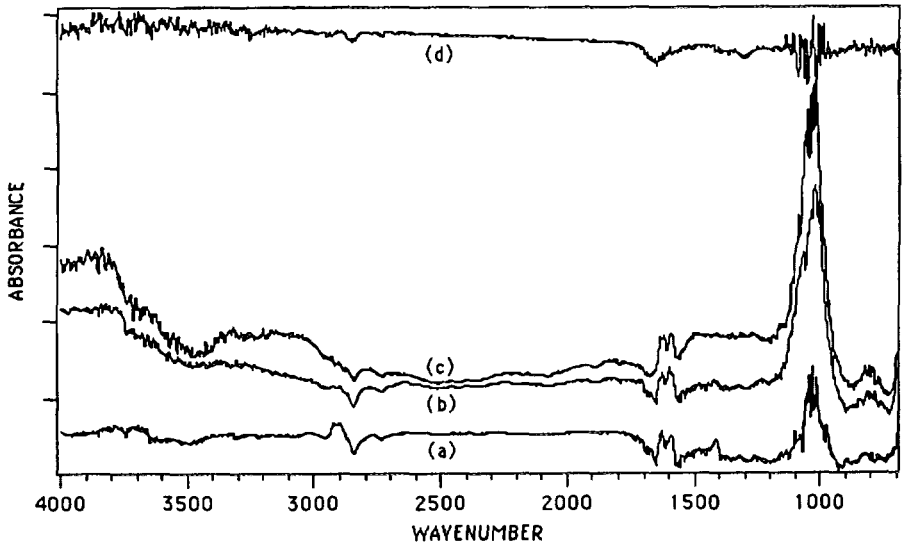

FIG. 10. DRIFT spectra of α-Al_2O_3(U) in He (sample after kinetic study) showing incremental changes with time: (a) after first 30-min period at 493 K in He; (b) after second 30-min period; (c) after third 30-min period; and (d) after fourth 30-min period. The reference spectrum in each case is that of the preceding case, i.e., the spectrum for (b) is referenced to that of (a), etc. Scale: 1 division = 0.02 absorbance unit.

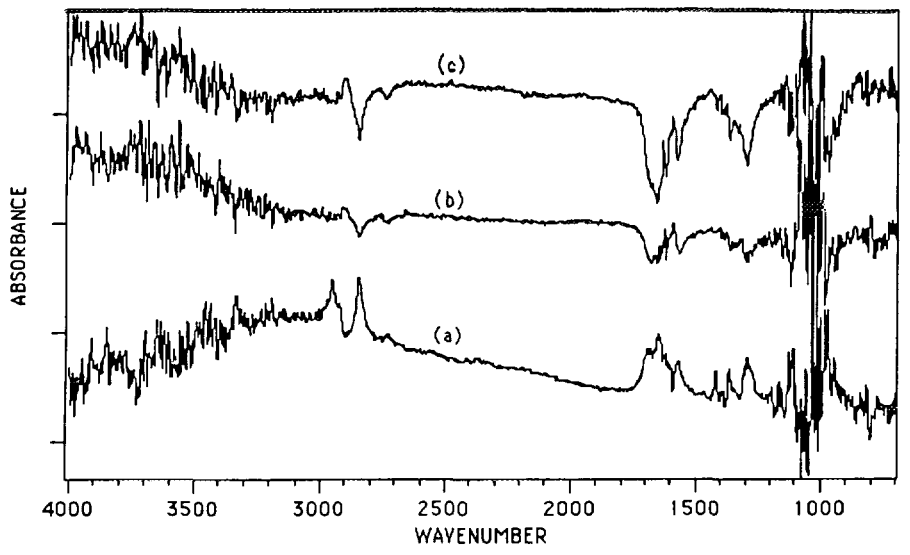

FIG. 11. DRIFT spectra of α-al$_2$O$_3$(U) (sample after kinetic study) at 493 K under He: (a) after 10 doses of H_2CO; (b) 20 min after last dose of H_2CO; and (c) after 60 min. The reference spectrum for (a) is that of the sample before dosing H_2CO, and the reference spectrum for (b) and (c) is that of the sample after the last dose of H_2CO. Scale: 1 division = 0.01 absorbance unit.

the previous pretreatment in flowing He at 493 K, the band at 1030 cm^{-1} suggests the formation of methoxy groups and those at 1620, 1595, and 1415 cm^{-1} correspond to formate species, while the decrease in band strength at 2850 and 2730 cm^{-1} implies the loss of dioxymethylene species (Fig. 10). These spectra are referenced to the used catalyst covered with surface species; consequently, the absence of bands in the 2800–3000 cm^{-1} region does not mean that they do not exist—just that there is little change. The broad band at 1660 cm^{-1} in Fig. 11 is most likely due to the scissors-bending mode of molecularly adsorbed water (33, 34), which had desorbed during the pretreatment as well as after the last dose of H_2CO, but readsorbed during the introduction of H_2CO due to its presence in the paraformaldehyde. The existence of molecularly adsorbed water was initially due to the air exposure of the used sample at room temperature after the kinetic studies. Dosing H_2CO at 493 K produced only dioxymethylene species, in contrast to the fresh sample on which formate species were dominant. This suggests the possibility that the formation of dioxymethylene is favored during H_2CO adsorption after surfaces are saturated with formate species; however, species like POM and methoxy groups are also possible since their characteristic bands are either similar to those of dioxymethylene or lie in the noisy 1000–1200 cm^{-1} region created by the high absorbance of the alumina itself.

The spectra for H_2CO adsorption on fresh 0.83% Ag/α-Al_2O_3(U) after pretreatment were similar to those on α-Al_2O_3(U), and no additional bands were observed for H_2CO adsorption on the Ag surface because of the low Ag loading and the strong interaction between H_2CO and alumina (20). However, after H_2CO adsorption in He and the introduction of O_2 at 493 K, the evolution of bands did not show the growth of formate groups, but instead a band formed at 1640 cm^{-1} during the early stages while band intensity decreased between 1400 and 1600 cm^{-1}, as shown in Fig. 12. After 1 h significant losses of band strength at 1620, 1595, 1460, and 1370 cm^{-1} had occurred (Fig. 12c), which were not observed with pure α-Al_2O_3(U). The loss of the doublet at 1620 and 1595 cm^{-1} and the bands at 1370 and 1460 cm^{-1} indicates a depletion of formate and dioxymethylene species from the surface. The initial spectra are possibly the combination of two reactions—the formation of formate groups on the alumina surface and the oxidation of formate ions at the Ag surface. The band at 1640 cm^{-1} is also attributed to formate species on the alumina surface, perhaps on different sites. From this result, it seems that formate groups on the alumina surface may migrate to the Ag surface, where oxidation occurs at 493 K; however, gas-phase oxidation products like CO_2 were not observed in these spectra.

DISCUSSION

Formaldehyde oxidation on supported Group VIII and Group IB metals has been investigated in the past to a limited extent (2–6). McCabe and Mitchell studied this reaction over a variety of alumina-supported metals and demonstrated that Pt had the highest activity while Ag showed relatively lower activity which could be enhanced by adding Pd (2). On the other hand, when dispersed on cerium oxide, Ru was more active than Pd and Pt, and this activity was associated with the capability of ruthenium

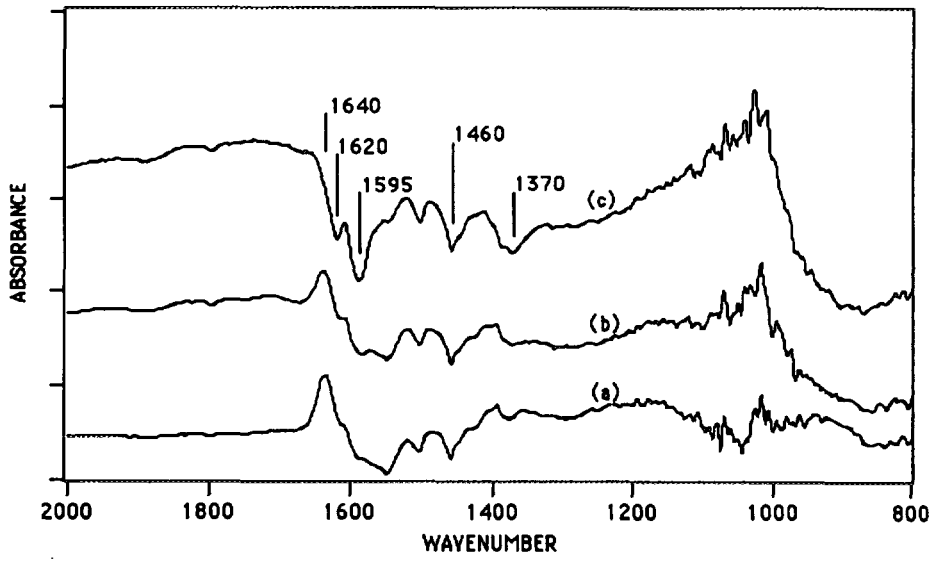

FIG. 12. DRIFT spectra of 0.83% $Ag/\alpha\text{-}Al_2O_3(U)$ at 493 K after exposure to 12 pulses of formaldehyde in He: (a) 5 min after exposure to O_2; (b) after 20 min; and (c) after 60 min. The reference spectrum is that of the sample after the last dose of H_2CO in He. Scale: 1 division = 0.02 absorbance unit.

oxide to transfer its lattice oxygen to formaldehyde (3). An activity comparable to that of Ru/CeO_2 was reported in a recent study of H_2CO oxidation over Ag/CeO_2 under similar reaction conditions (4). Sodhi *et al.* examined this reaction over Pt/Al_2O_3 and concluded that the conversion of H_2CO could be promoted and the production of CO reduced by increasing Pt loading, the oxygen/formaldehyde ratio, and the reaction temperature (5). Furthermore, the effect of pretreatment on liquid-phase H_2CO oxidation over Pt/TiO_2 catalysts has been studied to elucidate the influence of strong metal–support interactions (6). It should be noted that the activity of the pure support was not determined in these studies except in those of Imamura *et al.* As shown by our results, this contribution can be large; consequently, these relative activities must be accepted cautiously.

This study has shown that both Ag powder and $\alpha\text{-}Al_2O_3$ exhibit activity for H_2CO oxidation above 473 K, but only the supported Ag samples were active enough to oxidize H_2CO below 473 K, although significant deactivation was observed. Since neither Ag powder nor $\alpha\text{-}Al_2O_3$ showed any detectable activity below 473 K, the activity at these lower temperatures could be due to certain active sites which are only available on small Ag crystallites because the total Ag surface area in each reactor charge was similar. Among the three supported Ag catalysts showing activity below 473 K, the Ag/SiO_2 sample showed one of the highest TOFs and the lowest activation energy, though its deactivation was also the most pronounced. This deactivation is possibly due either to the polymerization of formaldehyde to cover part of the Ag surface, or to poisoning of active sites by certain strongly bound species, or to pore blockage by polymerized species.

Silica is not active for H_2CO oxidation; therefore, the activity of the Ag/SiO_2 sample is associated with the Ag surface. Compared to the results above 473 K for the Ag powder, the Ag/SiO_2 sample had a higher TOF, a lower E_a value, considerable deactivation, and reaction orders of 0.32 for both O_2 and H_2CO, compared to the first- and zero-order dependencies on O_2 and H_2CO, respectively, of Ag powder, thus indicating that significant differences in kinetic behavior exist between small 5-nm Ag crystallites and 10-μm Ag crystallites. The activity of the used Ag/SiO_2 sample was much lower than that of the fresh sample if the Arrhenius plot of the fresh sample is extrapolated to temperatures above 473 K; however, the apparent activation energy was similar in both temperature regimes.

The (HSA) $\alpha\text{-}Al_2O_3$ samples exhibited activities for H_2CO oxidation that were similar to, but somewhat lower than, those of the corresponding $Ag/\alpha\text{-}Al_2O_3$ catalysts. Deactivation also occurred on these samples, which again may have been due to polymerization of H_2CO to block active sites. CO was observed as an additional oxidation product during H_2CO oxidation on the $\alpha\text{-}Al_2O_3$ and $Ag/\alpha\text{-}Al_2O_3$ samples, and this reaction can be attributed to the decomposition of formate species on the alumina surface to release gas-phase CO and generate hydroxyl groups. In the presence of Ag the selectivity to CO_2 increased, thus implying that CO may be oxidized to CO_2 on Ag under reaction conditions or that a different reaction is occurring on the Ag to form CO_2, as the activity for H_2CO

oxidation to CO_2 on α-Al_2O_3 was consistently lower than that on the Ag/α-Al_2O_3 catalysts. Compared to the partial pressure dependencies of H_2CO oxidation over the Ag powder and the supported Ag, those for α-Al_2O_3 showed a weaker dependence on O_2 but a stronger one on H_2CO. On the other hand, since both Ag powder and the α-Al_2O_3 were active for H_2CO oxidation, the kinetic behavior of the Ag/α-Al_2O_3 samples is obviously a combination of the activities of both the Ag and the alumina, thus it is not surprising that their reaction orders fell between those for Ag powder and those for α-Al_2O_3.

Only CO_2 was formed during H_2CO oxidation on Ag powder or silica-supported Ag, whereas significant CO formation was observed in the presence of (HSA) α-alumina; therefore, CO formation is directly related to H_2CO oxidation over alumina surfaces rather than Ag surfaces. Any effect due to Ag crystallite size is ruled out based on the selectivity results in Table 3 and similar Ag crystallite sizes for the 1.5% Ag/SiO_2 and the two Ag/α-Al_2O_3 catalysts. Reaction mechanisms for H_2CO oxidation have been proposed for Pt and Pd catalysts (2, 5, 7). The proposed reaction pathway on Pt includes the decomposition of adsorbed H_2CO to adsorbed CO and H_2 (or adsorbed H) followed by oxidation or desorption of CO, with CO oxidation as the rate-determining step (5, 7). This mechanism was supported by the presence of CO in the product stream and further reinforced by the similarities in kinetic behavior between H_2CO and CO oxidation on Pt (7). However, the decomposition of adsorbed H_2CO prior to oxidation does not seem to occur on Ag surfaces, as evidenced by the formate species at 493 K identified in the IR spectra and the absence of CO as a reaction product over Ag powder and silica-supported Ag. Formaldehyde oxidation on Pd has been proposed to occur via a direct interaction of H_2CO with adsorbed atomic oxygen to form CO_2 and HO_2 (2). In addition this mechanism does not accurately describe H_2CO oxidation on Ag surfaces because the IR study of 16.65% Ag/SiO_2 showed that H_2CO adsorption resulted in formate species which could be oxidized at higher temperatures to give CO_2; therefore, formate species are a more probable intermediate during H_2CO oxidation on Ag.

Past studies of H_2CO and formic acid adsorption on Ag(110) can shed some light on the reaction pathway of H_2CO oxidation on Ag surfaces (19, 21, 35, 36). An EELS study of H_2CO adsorption on oxygen-covered Ag(110) has identified adsorbed species at different temperatures (19). Both dioxymethylene and polymerized H_2CO were present at 200 K, while the dominant species at 225 K was dioxymethylene, which completely decomposed to give formate groups at 250 K. The resulting formate groups further decomposed at 410 K to produce CO_2 and H_2. In our study, the IR results show stable formate species, which is consistent with the EELS study, though the continued existence of formate species at 493 K may be due to formate species strongly bound to defect sites on the Ag surface. The formate species generated from the interaction between adsorbed H_2CO and oxygen atoms chemisorbed on the Ag surface were found to be identical to those resulting from formic acid adsorption on clean Ag (35); therefore, the oxidation of formate species on Ag is applicable to H_2CO oxidation. Sault and Madix reported that in the presence of oxygen the decomposition temperature of formate species decreases due to the attack of adsorbed oxygen on the formate group, and the interaction between a formate ion and a neighboring oxygen atom or hydroxyl group releases CO_2 and forms a hydroxyl group or water (36). This behavior was also observed in a recent IR study of formic acid adsorption on Ag/SiO_2 (22).

The studies of H_2CO adsorption on Ag(110) combined with this IR study of Ag/SiO_2 suggest that the formate group is the most stable organic intermediate and its rate of decomposition to produce CO_2 could control the rate of H_2CO oxidation. Adsorbed H_2CO and dioxymethylene can easily transform into formate species under reaction conditions; therefore, a Langmuir–Hinshelwood (L–H) model with the decomposition of formate species as the rate determining step (RDS) was considered to describe H_2CO oxidation over Ag. However, this rate expression gave a poor correlation between the data and this model and, in addition, it could not be simplified to give the zero-order dependence on H_2CO and first-order dependence on O_2 that was obtained with Ag powder (20). Due to these two limitations, this L–H model does not describe the predominant reaction mechanism for H_2CO oxidation on these Ag catalysts. Other L–H models were also unsuccessful (20).

Only one general model was found that successfully fit all the data—one similar to that proposed by Mars and van Krevelen for hydrocarbon oxidation in which there is no rate-determining step but rather two irreversible steps that control the rate of reaction, i.e., the rate of reduction of an oxide catalyst surface is equal to its rate of reoxidation (37). Such an approach, which assumes that the rate of CO_2 formation (i.e., H_2CO decomposition—step [1e] below) is equal to the rate of oxygen adsorption (step [1a] below) and that all other steps are in quasi-equilibrium, generates the sequence of elementary steps

$$O_{2(g)} + 2\,S \xrightarrow{k_{O_2}} 2\,O\text{–}S \qquad [1a]$$

$$H_2CO_{(g)} + S \xleftrightarrow{K_{H_2CO}} H_2CO\text{–}S \qquad [1b]$$

$$H_2CO\text{–}S + O\text{–}S \xleftrightarrow{K_1} H_2CO_2\text{–}S + S \qquad [1c]$$

$$H_2CO_2\text{–}S + O\text{–}S \xleftrightarrow{K_2} HCO_2\text{–}S + HO\text{–}S \quad [1d]$$

$$HCO_2\text{–}S + O\text{–}S \xrightarrow{k_3} OH\text{–}S + CO_{2(g)} + S \quad [1e]$$

$$2\,HO\text{–}S \xleftrightarrow{1/K_{H_2O}} H_2O_{(g)} + O\text{–}S + S, \quad [1f]$$

where S represents an empty active site, k_{O_2} and k_3 are rate constants, and K_{H_2CO}, K_1, K_2, and K_{H_2O} are equilibrium constants. Step [1e] is consistent with the results of Sault and Madix (36). The assumptions that formate groups are the dominant organic reaction intermediate, which is supported by our DRIFTS data, and that adsorbed O is the most abundant surface intermediate give a site balance of $L = [S] + [HCO_2\text{–}S] + [O\text{–}S]$, which simplifies to $L = [S] + [O\text{–}S]$ and results in the rate expression

$$r = \frac{L\,k_{O_2}P_{O_2}}{[1 + k_{O_2}^{0.4}\,K_{H_2O}^{0.1}(k_3\,K_{H_2CO}\,K_1\,K_2)^{-0.4}\,P_{H_2O}^{0.1}P_{O_2}^{0.4}\,P_{H_2CO}^{-0.4}]^2}$$

$$= \frac{k'_{O_2}\,P_{O_2}}{[1 + K\,P_{H_2O}^{0.1}\,P_{O_2}^{0.4}\,P_{H_2CO}^{-0.4}]^2} \cong \frac{k'_{O_2}\,P_{O_2}}{[1 + K'\,P_{O_2}^{0.4}\,P_{H_2CO}^{-0.4}]^2} \quad [2]$$

where K is a parameter containing six constants. This equation, with only two fitting parameters, was rearranged to a linear form and, assuming the weak dependence on water to be relatively constant, it provided extremely good fits and correlation coefficients near unity. Furthermore, if the fractional coverage of both reactive oxygen and formate groups is low, Eq. [2] simplifies to give a first-order dependence on P_{O_2} and a zero-order dependence on P_{H_2CO}; therefore, it can also successfully describe the data for Ag powder. The parameters obtained from these linear regressions are listed in Table 5, and they are quite consistent, particularly the rate constants for O_2 adsorption, which vary by only a factor of two. Furthermore, the preexponential factor of the rate constant for oxygen adsorption, k_{O_2}, is around 20 cm s^{-1} for Ag powder, which is below the maximum value of 10^4 cm s^{-1} expected for adsorption on a clean surface (38). This model was also fitted to the partial pressure dependency data for α-Al_2O_3 and Ag/α-Al_2O_3, and correlations were surprisingly good though it is not known to what extent dissociative adsorption of oxygen occurs on alumina surfaces. Table 5 also lists these parameters, which again are remarkably consistent. The L–H model that assumes decomposition of formate species as the RDS again failed to fit the data for the α-Al_2O_3 and Ag/α-Al_2O_3 samples (20). However, a model similar to the preceding sequence except that step [1e] invokes an empty site to form an H–S species gives an equally good fit for the data for all the catalysts.

TABLE 5

Kinetic Parameters Obtained from Fitting of the Rate Expression (Eq. [2])

Catalyst	k'_{O_2}	$K\,P_{H_2O}^{0.1}$	r^{2a}
Ag powder	2.1[b]	—	
1.5% AG/SiO_2	2.6[b]	0.32	0.989
0.83% Ag/α-Al_2O_3(U)	1.8[c]	0.30	0.965
0.71% Ag/α-Al_2O_3(G)	3.8	0.60	0.958
α-Al_2O_3(U)	3.1[c]	0.65	0.955
α-Al_2O_3(G)	2.8[c]	0.78	0.987

Note. T = 493 K.
[a] Correlation coefficient.
[b] Units (1/s · Torr × 10^5).
[c] Units (mol/g · s · Torr × 10^9).

Numerous kinetic studies of gas-phase H_2CO oxidation above 523 K have been reported (39), however, few kinetic data are available in the literature for the catalytic combustion of H_2CO. The only work reporting kinetic data for H_2CO oxidation is that of McCabe and McCready, who utilized a Pt wire and reported an apparent activation energy of 40 kJ mol^{-1}, a H_2CO pressure dependency at 430 K near −0.75, and an O_2 pressure dependency around 1.5 (7). Our values for Ag powder are different in all aspects; thus, the reaction mechanisms over Pt and Ag are very likely different, as discussed previously, and it is evident that the aforementioned model for Ag cannot provide agreement with the partial pressure dependencies of this reaction on Pt. Unfortunately, an accurate comparison of specific activities of different metals is not possible because the metal surface areas and TOFs have not been previously reported and the contributions of alumina supports were not measured. Estimates per gram of metal (20) indicate our Ag/α-Al_2O_3 catalysts are 2–4 times less active than the Ag/γ-Al_2O_3 catalyst used by McCabe and Mitchell and an order of magnitude less active than their γ-Al_2O_3-supported Pt, Pd, and Rh catalysts (2). However, a greater activity on the γ-Al_2O_3 surface could account for this.

The kinetic behavior of H_2CO oxidation over alumina has not been addressed in the literature, but the use of Al_2O_3 to adsorb H_2CO has been reported (40). In either oxidation or adsorption of H_2CO on aluminas, a fundamental understanding of the adsorbed H_2CO species is required. The IR study of H_2CO adsorption on aluminas done by Busca *et al.* covered a wide temperature range and provides information about the evolution of adsorbed species on alumina surfaces (17). At temperatures as low as 170 K, physisorbed H_2CO was observed while slow warming to 200 K led to the identification of POM, dioxy-

methylene, and coordinated H_2CO species, and further warming to room temperature created formate ions and methoxy groups. The formation of formate and methoxy groups was suggested to come from disproportionation of dioxymethylene although direct oxidation of dioxymethylene to formate was not excluded. Formate species were also observed on alumina by Greenler during methanol adsorption above 443 K (23), and this was attributed to oxidation of methoxy groups by oxygen atoms from the alumina surface (41). Further oxidation of formate species by lattice oxygen atoms may be possible as carbonate groups on Fe_2O_3 surfaces have been reported (42). In our IR study of H_2CO adsorption on (HSA) α-alumina, the decomposition of dioxymethylene species to formate and methoxy was also observed at 303 K, which is consistent with previous studies (17, 24). The kinetic study shows formation of both CO_2 and CO, which is attributed to separate reactions for the oxidation and decomposition of formate groups, respectively.

SUMMARY

This kinetic study has shown that both Ag and (HSA) α-alumina are active for H_2CO oxidation above 473 K. Only complete combustion products were observed over Ag powder and silica-supported Ag while CO was also formed over the (HSA) α-aluminas. The reaction orders for CO_2 formation on Ag powder were unity for O_2 and zero for H_2CO but those for the pure aluminas were around 0.1 for O_2 and between 0.3 and 0.6 for H_2CO. The reaction orders for the supported Ag catalysts above 473 K were around 0.3 for both O_2 and H_2CO. The supported Ag catalysts were also active below 473 K but strong deactivation occurred, and the activities could not be recovered by utilizing another pretreatment. TOFs for H_2CO oxidation are reported for the first time. A sequence of elementary steps assuming the rate of O_2 adsorption to be equal to the rate of formate decomposition to CO_2 was proposed, and this model gave an excellent fit for the data for all catalysts. This reaction sequence is also consistent with the IR study because formate groups are assumed to be the major organic intermediate.

The IR study showed that a strong interaction occurs between H_2CO and the (HSA) α-alumina. Formate groups were the dominant species in the temperature range studied and dioxymethylene species also existed in significant amounts at 303 K, and the presence of POM and methoxy groups on the alumina surfaces could not be excluded. The evolution of IR bands after the last dose of H_2CO revealed the growth of formate species and the disappearance of dioxymethylene species, suggesting the conversion of dioxymethylene to formate groups. The spectra after H_2CO adsorption on alumina-supported Ag were similar to those for the (HSA) α-alumina. The major difference with the Ag/α-Al_2O_3 samples was a decrease in band strength associated with formate groups after exposure to oxygen at 493 K, which implies the oxidation of formate species at the Ag surface. Since no bands were observed after H_2CO adsorption on silica, the IR bands from silica-supported Ag are associated only with the Ag surface. Formate species were the only adsorbed species that could be observed after the exposure of H_2CO to oxygen-covered Ag surfaces, and gas-phase CO_2 was detected after the introduction of O_2 at 493 K.

ACKNOWLEDGMENTS

The FTIR studies were conducted with a DRIFTS system acquired with an NSF equipment grant (CTS-9311087). Partial support from NSF Grant CTS-9019612 and the Mobil Corporation is also gratefully acknowledged.

REFERENCES

1. Swenberg, J. A., Kerns, W. D., and Mitchell, R. I., *Cancer Res.* **40,** 3398 (1980).
2. McCabe, R. W., and Mitchell, P. J., *Appl. Catal.* **44,** 73 (1988).
3. Imamura, S., Uematsu, Y., Utani, K., and Ito, T., *Ind. Eng. Chem. Res.* **30,** 18 (1991).
4. Imamura, S., Uchihori, D., Utani, K., and Ito, T., *Catal. Lett.* **24,** 377 (1994).
5. Sodhi, D., Abraham, M. A., and Summers, J. C., *J. Air Waste Manage. Assoc.* **40,** 352 (1990).
6. Jakse, F. P., Friedman, R. M., Delk, F. S., II, and Bulock, J. W., *Appl. Catal.* **14,** 303 (1985).
7. McCabe, R. W., and McCready, D. F., *Chem. Phys. Lett.* **111,** 89 (1984).
8. Foster, J. J., and Masel, R. I., *Ind. Eng. Chem. Prod. Res. Dev.* **25,** 563 (1986).
9. Mao, C.-F., and Vannice, M. A., *Appl. Catal. A* **122,** 61 (1995).
10. Mao, C.-F., and Vannice, M. A., *Appl. Catal. A* **111,** 151 (1994).
11. Li, X., and Vannice, M. A., *J. Catal.* **151,** 87 (1995).
12. Seyedmonir, S. R., Strohmayer, D. E., Geoffroy, G. L., and Vannice, M. A., *Adsorpt. Sci. Technol.* **1,** 253 (1984).
13. Walker, J. F., "Formaldehyde." Reinhold, New York, 1953.
14. Venter, J. J., and Vannice, M. A., *Appl. Spectrosc.* **42,** 1096 (1988).
15. Meima, G. R., Knijff, L. M., van Dillen, A. J., Geus, J. W., and van Buren, F. R., *J. Chem. Soc. Faraday Trans. 1* **85,** 293 (1989).
16. Meima, G. R., Hasselaar, M., van Dillen, A. J., van Buren, F. R., and Geus, J. W., *J. Chem. Soc. Faraday Trans. 1* **85,** 1267 (1989).
17. Busca, G., Lamotte, J., Lavalley, J.-C., and Lorenzelli, V., *J. Am. Chem. Soc.* **109,** 5197 (1987).
18. Carver, C. D., "Infrared Spectra of Regulated and Major Industrial Chemicals." Coblentz Society, Inc., Kirkwood, MO, 1983.
19. Stuve, E. M., Madix, R. J., and Sexton, B. A., *Surf. Sci.* **119,** 279 (1982).
20. Mao, C.-F., Ph.D. thesis, Pennsylvania State University, 1994.
21. Sexton, B. A., and Madix, R. J., *Surf. Sci.* **105,** 177 (1981).
22. Millar, G. J., Metson, J. B. Bowmaker, G. A., and Cooney, R. P., *J. Catal.* **147,** 404 (1994).
23. Nakamoto, K., "IR and Raman Spectra of Inorganic and Coordination Compounds," Chap. 3. Wiley, New York, 1986.
24. Greenler, R. G., *J. Chem. Phys.* **37,** 2094 (1962).
25. Trillo, J. M., Munuera, G., and Criado, J. M., *Catal. Rev.* **7,** 51 (1972).

26. Lavalley, J. C., Lamotte, J., Busca, G., and Lorenzelli, V., *J. Chem. Soc. Chem. Commun.*, 1006 (1985).
27. Raval, R., and Munso, S., *J. Electron Spectrosc. Relat. Phenom.* **64/65,** 461 (1993).
28. Mikawa, Y., Brasch, J. W., and Jakobsen, R. J., *J. Mol. Spectrosc.* **24,** 314 (1967).
29. Bratoz, S., Hadzi, D., and Sheppard, N., *Spectrochim. Acta* **8,** 249 (1956).
30. Novak, A., and Whalley, E., *Trans. Faraday Soc.* **55,** 1484 (1959).
31. Tadokoro, H., Kobayashi, A., Kawaguchi, Y., Sobajima, S., and Murahashi, S., *J. Chem. Phys.* **35,** 369 (1961).
32. Shimomura, M., and Iguchi, M., *Polymer* **23,** 509 (1982).
33. Morterra, C., Ghiotti, G., Garrone E., and Boccuzzi, F., *J. Chem. Soc. Faraday Trans. 1* **72,** 2722 (1976).
34. Borello, E., Gatta, G. D., Fubini, B., Morterra C., and Venturello, G., *J. Catal.* **35,** 1 (1974).
35. Barteau, M. A., Bowker, M., and Madix, R. J., *Surf. Sci.* **94,** 303 (1980).
36. Sault, A. G., and Madix, R. J., *Surf. Sci.* **176,** 415 (1986).
37. Mars, P., and van Krevelen, D. W., *Chem. Eng. Sci. Spec. Suppl.* **3,** 41 (1954).
38. Boudart, M., and Djéga-Mariadassou, G., "Kinetics of Heterogeneous Catalytic Reactions." Princeton Univ. Press, 1984.
39. Griffiths, J. F., and Skirrow, G., *Oxid. Combust. Rev.* **3,** 47 (1968).
40. Solov'ev, S. A., Vol'fson, V. Ya., and Vlasenko, V. M., *Zh. Prikl. Khim.* **60,** 2137 (1987).
41. Hertl, W., and Cuenca, A. M., *J. Phys. Chem.* **77,** 1120 (1973).
42. Busca, G., and Lorenzelli, V., *J. Catal.* **66,** 155 (1980).